Journal of Marine Research, 60, 699–723, 2002

Internal gravity wave frequencies and wavenumbers from single point measurements over a slope

by S. A. Thorpe[1,2] and L. Umlauf[3]

ABSTRACT

It is shown that information about the intrinsic frequency of internal inertial gravity waves, together with their vector wavenumber and their steepness spectrum, may be derived using data from a meter recording current and temperature just above a uniform sloping boundary. The analysis assumes that, over the periods of time in which estimates are made, the local mean buoyancy frequency, N, and temperature gradient are uniform, and the bottom slope, α, is constant over the scale of the observed waves and is known. It is further assumed that, during short periods of analysis, the internal wave field is dominated by waves having a single wavenumber vector at each frequency. Measurements of the temperature and up-slope current spectra can be used to determine the intrinsic frequency and the along-slope wavenumber, l, of the waves provided the mean along-slope current, V, is non-zero. If the internal wave field near the sloping boundary is composed of perfectly reflecting wave rays, it is found that the ratio, R, of the potential energy density of the waves of given frequency to that of their kinetic energy depends on α and on the ratio, l/k, of waves in the reflecting wave field, where k is the up-slope wavenumber. Since l is already determined if $V \neq 0$, k may be estimated from the measured R. The third component of wavenumber, m, normal to the slope is found from the dispersion relation. The estimated values may be used to test assumptions of small wave steepness and the uniformity of buoyancy frequency over the vertical scale of the waves.

Problems of application are revealed by using the analysis on data collected from a mooring located within the hyperlimnion on the sloping side of Lake Geneva. Whilst the along-slope wavenumbers and corresponding intrinsic frequencies can be found, it proves impossible to derive estimates of wave directions for waves in the subcritical frequency range of group velocities having angles to the horizontal, β, less than α, and supercritical waves ($\beta > \alpha$) have inferred wavelength which violate assumptions of the vertical uniformity of N. It is inferred that in the lake the wave propagation is dominated by waves with a modal structure rather than rays, even near the buoyancy frequency. The methodology should however be applicable in the deep ocean, subject to the various assumptions which are made.

Fundamental questions are raised about the directional characteristics and persistence of internal waves near sloping boundaries which deserve further investigation in view of their possible relation to mixing.

1. SOES, Southampton Oceanography Centre, European Way, Southampton, SO14 3ZH, United Kingdom.

2. Address for correspondence: 'Bodfryn,' Glanrafon, Llangoed, Anglesey, LL58 8PH, United Kingdom. ***email: oss413@sos.bangor.ac.uk***

3. Laboratoire Recherches Hydraulique, Ecole Polytechnique Fédérale de Lausanne, CH-1015, Lausanne, Switzerland.

1. Introduction

The internal slope boundary layer is the region of the ocean or of lakes within which the ambient internal inertial gravity wave field is modified by the presence of sloping, and sometimes rough, topography. It may contain an internal surf zone of relatively high wave dissipation. In the abyssal ocean and the hypolimnion of lakes, it is a region of wave reflection, where wavenumbers are changed and waves are amplified. In his illuminating study of the reflection of internal waves propagating as rays in the deep ocean, Eriksen (1982, 1985) shows that shear is particularly enhanced when the internal wave frequencies, σ, are close to the critical frequency on the slope, σ_c, given by

$$\sigma_c^2 = N^2 \sin^2 \alpha + f^2 \cos^2 \alpha, \tag{1}$$

or when the inclination of the wave group velocity vector to the horizontal, β, is equal to α, the angle of inclination of the locally plane bottom to the horizontal. In (1), N is the buoyancy frequency, assumed locally uniform, and f is the Coriolis frequency. There are also many nonlinear effects associated with wave reflection, such as wave steepening and front formation (Thorpe, 1992, 1999a), the generation of along-slope currents (Thorpe, 1997, 1999b; Dunkerton *et al.,* 1998; Zikanov and Slinn, 2001) and the ejection of mixed water from the boundary into the ocean interior (Thorpe, 1999c, 2001a). Changes to the wave field may lead to the enhanced diapycnal flux so often observed near slopes (e.g. see Ledwell and Hickey, 1995; Ledwell and Bratkovich, 1995, Toole *et al.,* 1997; Imberger and Ivey, 1993; Eriksen, 1998; Morris *et al.,* 2001) and is one reason why the internal slope boundary layer is so important.

Very little is known by direct measurements of the internal wave field near slopes and almost nothing of its directional properties and wavenumber spectra. This is partly because of the apparent necessity to deploy complex or extensive instrument arrays. There is, in particular, a need for more information about the variability of the directional properties and wavenumbers of internal waves in the ocean and in lakes to help identify their cause or source and their relation to the wind field and to investigate how they respond to, or generate, variations in along-slope currents. This forms a motivation for this study.

We show that, in some regions of the ocean and possibly in deep lakes, it is possible to infer some aspects of the wave field economically using measurements from a *single* moored current meter recording the horizontal component of current and the temperature variations, perhaps augmented by sparse observations of the mean vertical temperature gradient and buoyancy frequency at the mooring. The analysis supporting this conclusion is described in Section 2. Particular attention is drawn in Section 2f to the assumption that, over sufficiently short periods of time, there are waves which dominate the wave spectra near a sloping boundary, and to the similarities and differences between surface and internal waves near sloping boundaries. Data from a shallow mooring deployed in Lake Geneva are described in Section 3 and used to reveal and examine some of the problems encountered in applying the analysis, especially when the data are from a location which is relatively close to the surface or thermocline.

2. Analysis

a. A relation between observed and intrinsic frequencies, and the along-slope wavenumber

We consider a uniform slope which bounds a deep stratified ocean or lake. The condition of uniformity requires that the slope is uniform over the scale of the waves. We exclude here the possibility of slope roughness perturbing the mean flow to generate waves or eddies (Thorpe, 1996; MacCready and Pawlak, 2001) or interacting with the incident wave field to generate new wave components (Thorpe, 2001b). A current meter is located on a platform or mooring just above the bottom at a level which is not substantially affected by the frictional effects of the bottom or by the mixing which occurs there, but is sufficiently close that the component of velocity normal to the boundary is zero. It is supposed the instrument records a mean flow, V, in the y-direction along the slope, and that the measured fluctuations in current and temperature with intrinsic frequencies between the Coriolis frequency, f, and mean buoyancy frequency, N, are caused solely by internal waves. Vertical shear is ignored. It is further assumed that non-linear effects leading to fronts or other non-sinusoidal wave fluctuations are negligible in their contribution to spectra and that the local mean buoyancy frequency, N, is constant. These assumptions, allowing simplification in the theory described below, may be violated in some of the observations described in Section 3 and will be reviewed later.

A relation between the intrinsic frequency of the waves, σ, and the observed frequency, Σ, can be obtained by observing both the upslope velocity component and the temperature fluctuations, T. If the temperature is $T_0(Z) + T$, where T_0 is the mean temperature over some specified time period and Z is vertical then, neglecting turbulent and molecular diffusion, the conservation of temperature equation on a slope of angle α to the horizontal is

$$\partial T/\partial t + (V + v)\partial T/\partial y + u\partial T/\partial x = 0. \tag{2}$$

Here u is the upslope (x) component of current which has zero mean, and $V + v$ is the along-slope (y) flow. The component of flow, w, in the direction, z, normal to the slope, is zero at the boundary and is subsequently supposed to be negligibly small at the height of the measurements. Linearizing (2), the v term disappears and the $\partial T/\partial x$ term becomes sin $\alpha dT_0/dZ$ so:

$$\partial T/\partial t + V\partial T/\partial y + u \sin\alpha\, dT_0/dZ = 0. \tag{3}$$

If the motion field is described as one corresponding to a periodic disturbance with spectral components

$$u = u_0 \sin(kx + ly - \Sigma t) \qquad \text{and} \qquad T = T_1 \cos(kx + ly - \Sigma t), \tag{4}$$

where Σ is the frequency measured at the fixed moored current meter, then for each component (3) gives

$$T_1(\Sigma - Vl) = -u_0 \sin \alpha \, dT_0/dZ. \tag{5}$$

Now the intrinsic frequency of the internal waves, σ, is given by

$$\sigma = \Sigma - Vl, \tag{6}$$

so

$$u_0 = [-\sigma/(\sin \alpha \, dT_0/dZ)]T_1. \tag{7}$$

The frequency spectra of u and T as functions of the measured frequency, Σ, can be derived from the observations at the fixed location. But by (7), the frequency spectrum E_u of u, the upslope component of current, is equal to the frequency spectrum of temperature, E_T, times $[\sigma/(\sin \alpha \, dT_0/dZ)]^2$. If the slope of the bottom, α, and the mean vertical temperature gradient, dT_0/dZ, are known, then the ratio of the two spectra can be used to give σ as a function of frequency, Σ. [i.e., $(E_u/E_T)^{1/2} \sin \alpha (dT_0/dZ)$, which is equal to σ, may be plotted against Σ. The convention adopted here that σ is positive and that the direction of propagation of wave phase is prescribed by the sign and magnitude of the components of the wavenumber vector.] In principle, if the mean along-slope flow, V, is known and is non-zero, then, from (6), l can also be found as a function of the measured frequency, Σ, or of the intrinsic frequency, σ. In the (rare) conditions in which $V = 0$, there is no Doppler shift of the intrinsic wave frequency, the intrinsic frequency and the measured frequency are identical, and l cannot be determined directly from the measured quantities. If the velocity and temperature fluctuations arise from, say, turbulent eddies or boluses of fluid carried by the mean flow, rather than by internal waves, the Doppler shift will be zero and the relation between the fluctuation frequency and along-slope wavenumber is simply $\Sigma = Vl$.

The analysis applied above provides a method to derive information about the propagation direction of internal waves along the slope, which depends on the sign of l, and about the scale of the waves, $|l|$, as a function of their frequency. This may help, for example, to identify their sources. So far, nothing has been specified about the nature of the internal waves. They may have the character of wave modes with structure extending through the thermocline to the water surface or of wave rays with relatively small vertical scale propagating in the local region within which N is constant. The method described above applies to both wave types.

b. The velocity components

In principle (although, as we shall find later, perhaps not always in practice), by making an assumption about the nature of the waves it is possible to go further and to derive estimates of the wavenumbers of the internal waves on the slope. It is assumed that they have the character of wave rays propagating in a deep fluid of constant buoyancy frequency, N. Except perhaps at tidal frequencies, the assumption is likely to be generally valid in the abyssal ocean. Whilst there is evidence that the fine structure of temperature in

lakes is sometimes a consequence of such vertically propagating waves (Lazier, 1973), we shall find that the assumption fails when tested '*a posteriori*' in application to two short periods of lake data in section 3. Equations are now required for the wave velocity components.

We suppose that the Boussinesq approximation is valid. Consistent with the assumption that N is constant, the mean local density gradient is taken to be uniform so that, in the tilted x, y and z co-ordinates, the mean density is $\rho_0[1 - (N^2/g)(x \sin\alpha + z\cos\alpha)]$ where ρ_0 is the constant reference density and g is the acceleration due to gravity. Neglecting dissipation, the linearized x and y equations of the fluctuating motion are

$$\partial u/\partial t + V\partial u/\partial y - vf\cos\alpha = -(1/\rho_0)\partial p/\partial x - g\rho\sin\alpha/\rho_0 \tag{8}$$

and

$$\partial v/\partial t + V\partial v/\partial y + uf\cos\alpha = -(1/\rho_0)\partial p/\partial y, \tag{9}$$

respectively, where ρ is the density fluctuation from the mean density and p is the pressure. All the terms in w are zero on the slope; $w = 0$ at $z = 0$ for all x and y. Eliminating p between (8) and (9),

$$[\partial/\partial t + V\partial/\partial y](\partial u/\partial y - \partial v/\partial x) - f\cos\alpha(\partial u/\partial x + \partial v/\partial y) = -g(\partial\rho/\partial y)\sin\alpha/\rho_0. \tag{10}$$

The linearized density conservation equation is

$$[\partial/\partial t + V\partial/\partial y]\rho - uN^2\rho_0\sin\alpha/g = 0, \tag{11}$$

so taking the derivatives $[\partial/\partial t + V\partial/\partial y]$ of (10) and $\partial/\partial y$ of (11), and eliminating ρ we have

$$\begin{aligned}[\partial/\partial t + V\partial/\partial y]^2(\partial u/\partial y - \partial v/\partial x) - f\cos\alpha[\partial/\partial t + V\partial/\partial y](\partial u/\partial x + \partial v/\partial y)\\ = -N^2\sin^2\alpha\,\partial u/\partial y.\end{aligned} \tag{12}$$

Now suppose, as before, that u varies sinusoidally on the slope, so $u = u_0\sin(kx + ly - \Sigma t)$. The phase of v may differ so let

$$v = v_0\sin(kx + ly - \Sigma t) + v_1\cos(kx + ly - \Sigma t). \tag{13}$$

Using the dispersion relation for internal gravity waves

$$\sigma^2 = N^2\sin^2\beta + f^2\cos^2\beta \tag{14}$$

(Gill, 1982), where β is the inclination of the group velocity vector of waves of frequency σ to the horizontal, substituting in (12) for u and v, comparing coefficients of $\cos(kx + ly - \Sigma t)$ and $\sin(kx + ly - \Sigma t)$ and using (6), two equations for v_0 and v_1 are found in terms of u_0:

$$v_0/u_0 = q\gamma(1 - F^2)/(s^2 + F^2q^2\cos^2\alpha) \tag{15}$$

and

$$v_1/u_0 = -(F/s)\cos\alpha[s^2 + q^2(s^2 - \sin^2\alpha)]/(s^2 + F^2q^2\cos^2\alpha), \tag{16}$$

with $s = \sigma/N$, $F = f/N$, $q = l/k$ and $\gamma = \sin^2\beta - \sin^2\alpha$. The parameter q defines the direction of phase advance on the sloping boundary; $q = \tan\phi$, where ϕ is the angle between a constant phase line and the isobath on the slope. The parameter γ is positive for supercritical waves, negative for subcritical waves, and zero for waves which are critical on the slope, i.e. when $\sigma = \sigma_c$ (see 1) or when $\beta = \alpha$.

c. The ratio of PE to KE

We shall show how the ratio, R, of the potential energy density, PE, to the kinetic energy density, KE, of internal waves just above a slope provides information about the parameter $q = l/k$.

The PE density is $\rho_0 N^2\zeta^2/2$, where ζ is the vertical displacement of isotherms (Gill, 1982). Suppose the temperature gradient is constant. (This is already true in a fresh water lake when N is assumed to be constant provided the temperature range is small and the temperature not close to that of the maximum density near 4°C.) Then the displacement in the wave motion given by (4), is approximately

$$\zeta = T_1/(dT_0/dZ), \tag{17}$$

so, ignoring the factor $\rho_0/2$, the PE spectrum is equal to the spectrum of the temperature fluctuations, E_T, multiplied by $N^2/(dT_0/dZ)^2$.

The KE density of the fluctuations at a current meter above a uniformly sloping boundary is

$$KE = \rho_0(u_0^2 + v_0^2 + v_1^2)/2, \tag{18}$$

where ρ_0 is the reference density. Assuming that the current meter measures only the *horizontal* flow then, again ignoring the factor $\rho_0/2$, the KE spectra is found by taking the sum of the spectrum of the measured along-slope, v, flow components and $\sec^2\alpha$ times the spectrum of the measured horizontal component directed toward the slope.

It is therefore possible to calculate the ratio, R, of the potential energy, PE, to the kinetic energy density, KE, as a function of Σ, or using Section 2a, as a function of σ or (using 14) of β; $\beta = \sin^{-1}[(s^2 - F^2)/(1 - F^2)]^{1/2}$.

An analytical expression for the ratio R is available in deep water far from boundaries:

$$R = \sin^2\beta/(\sin^2\beta + 2F^2\cos^2\beta) \tag{19}$$

(Gill, 1982) which may be written

$$R = (s^2 - F^2)/\{F^2 + s^2[1 - 2F^2]\} \tag{20}$$

using the dispersion relation (14). R is equal to unity, giving equipartition of energy, if $F \ll s < 1$ (or $f \ll \sigma < N$). This is so unless β is very small when R tends to zero and (14)

implies that σ is near the inertial frequency. (Far from boundaries the motions in inertial waves are nearly in horizontal circles and the waves contain much less PE than KE so R is small.) If $F^2 \ll 1$, as is commonly the case in the ocean and in lakes, then (20) gives $R = 3/5$ when $\sigma = 2f$, and $R = 15/17 \approx 0.88$ when $\sigma = 4f$; the ratio, R, rapidly approaches 1 as σ increases above f, and remains close to 1 as σ increases to N.

Antenucci and Imberger (2001) have shown how potential energy and kinetic energy and their ratio, R, vary with location or Burger number for waves of different kinds and modes in circularly and elliptically shaped lakes, but of uniform finite depth. Sloping boundaries also change the ratio of the locally measured energy densities of internal waves. Near an inclined plane boundary, in the absence of rotation and along-slope mean flow, a sinusoidal movement of water up and down the slope over a distance $2A$ with frequency σ implies that the up-slope speed measured at a point may be written $-A\sigma \sin \sigma t$. The vertical displacement is $A \sin \alpha \cos \sigma t$. PE is therefore proportional to $N^2A^2 \sin^2 \alpha$ and KE to $A^2\sigma^2$, so that

$$R = \sin^2 \alpha / s^2. \tag{21}$$

When $F = 0$, the dispersion relation (14) gives $s^2 = \sin^2 \beta$, so

$$R = \sin^2 \alpha / \sin^2 \beta. \tag{22}$$

These ratios are different from those of about unity found in deep water remote from boundaries when $F = 0$. As σ tends to N, β tends to $\pi/2$, and R tends to $\sin^2 \alpha$ which will be small if the bottom slope is small.

The azimuthal angle of the incident waves, θ_I, is defined as the angle between the projection of the waves' group velocity onto the horizontal and a horizontal line normal to the isobaths of the slope and directed toward shallower water. Eq. (21) is appropriate for waves travelling directly toward the slope at zero azimuthal angle, so that the motion is all in a vertical plane normal to the slope (and therefore also normal to isobaths) and $q = 0$. The value of R can also be calculated for waves approaching and reflecting from a slope with nonzero values of q, that is with arbitrary azimuthal angles. Substituting for T_1 from (7) into (17) we obtain

$$PE = \rho_0 u_0^2 \sin^2 \alpha / 2s^2, \tag{23}$$

and so, using (18),

$$R = (\sin \alpha / s)^2 / [1 + (v_0/u_0)^2 + (v_1/u_0)^2]. \tag{24}$$

Substituting for v_0/u_0 and v_1/u_0 from (15) and (16) leads to an equation for R in terms of q, α, σ (or β), f and N, which can be written

$$\begin{aligned} R = \sin^2 \alpha (s^2 + F^2q^2 \cos^2 \alpha)^2 / [s^2(s^2 + F^2q^2 \cos^2 \alpha)^2 + q^2\gamma^2 s^2 (1 - F^2)^2 \\ + F^2 \cos^2 \alpha (s^2 + q^2 s^2 - q^2 \sin^2 \alpha)^2]. \end{aligned} \tag{25}$$

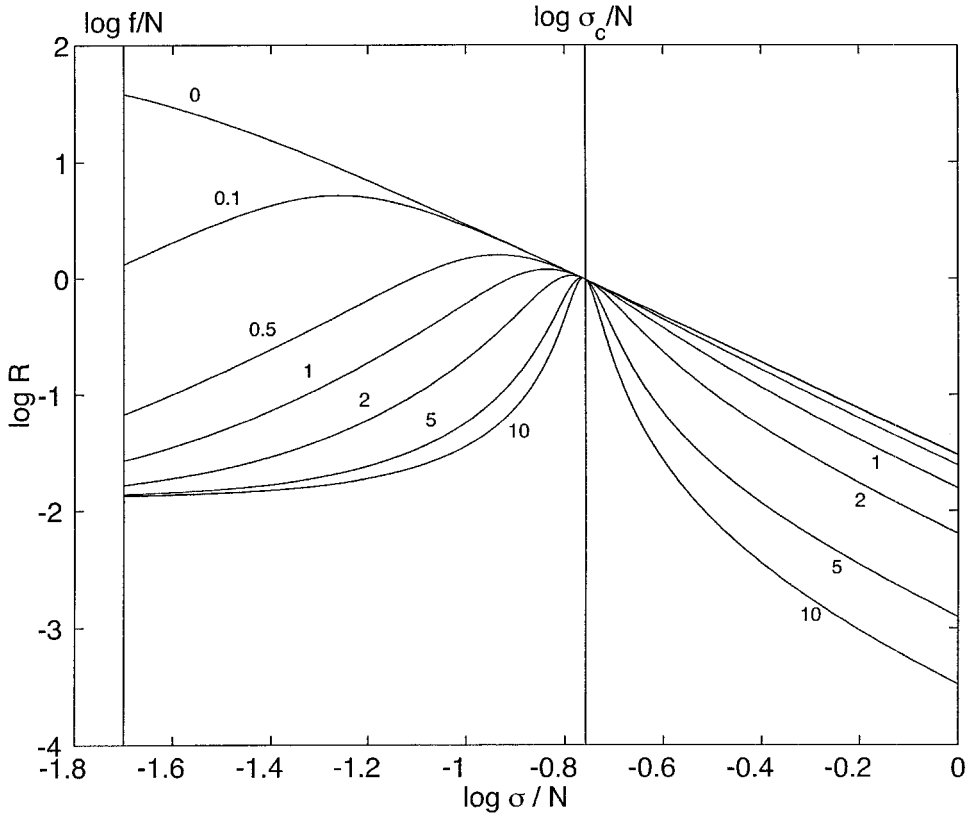

Figure 1. The ratio, R, of the potential energy density, PE, to the kinetic energy density, KE, as a function of $s = \sigma/N$ above a sloping boundary with $\alpha = 10°$ when $F = 0.02$ and at various values of q, shown by labels on the curves.

Figure 1 shows log (R) as a function of log(s) at various values of q when $\alpha = 10°$ and $F = 0.02$.

Eq. (25) can be simplified in some particular cases. When $q = 0$, i.e. for waves of normal incidence,

$$R = \sin^2 \alpha/(s^2 + F^2 \cos^2 \alpha), \tag{26}$$

giving (22) if $F = 0$, since $s^2 = \sin^2 \beta + F^2 \cos^2 \beta$. In consequence, the curve $q = 0$ in Figure 1 is almost linear with a -2 slope when $s \gg F$. If $\gamma = 0$ when the waves have critical frequency and $\beta = \alpha$, (25) reduces to

$$R = \sin^2 \alpha/(\sin^2 \alpha + F^2 \cos^2 \alpha), \tag{27}$$

independent of q (so q consequently cannot be determined exactly at the critical frequency by inverting 25) and the set of curves in Figure 1 all converge to a value of R close to unity as s tends to σ_c/N. When $F^2 \ll 1$, (25) gives

$$R = \sin^2\alpha \sin^2\beta/(\sin^4\beta + q^2\gamma^2), \tag{28}$$

decreasing as q increases. As expected, this leads to (22) when $q = 0$, i.e. when the waves are at zero azimuth or when l and θ_I are zero. With increasing β, R decreases from values of unity at $\beta = \alpha$ ($s = \sigma_c/N$) to $\sin^2\alpha/(1 + q^2\cos^4\alpha)$ (which is usually small and which is zero when $\alpha = 0$) when $\beta = \pi/2$ ($s = 1$). This contrasts with the behavior of R in deep water (see 20) where R is close to unity, and implies, as we shall see later in the data, that the KE and PE spectra measured close to a sloping boundary will usually have different power law relationships with σ, PE decreasing more rapidly than KE as σ increases.

In the inertial limit, $s = F$ (or $\sigma = f$), and when $F^2 \ll 1$, (25) gives

$$R = F^2(1 + q^2\cos^2\alpha)/(q^2\sin^2\alpha). \tag{29}$$

As σ tends to $f+$ in deep water, (20) shows that R tends to zero, in contrast to the behavior of (29) where R is finite and nonzero for small values of q and α.

If R is known as a function of β or σ from measurements as described above, we can solve (25) as a quadratic equation for the unknown value q^2:

$$\begin{aligned} &q^4F^2\cos^2\alpha\{F^2\cos^2\alpha[R^{-1}\sin^2\alpha - s^2] - [s^2 - \sin^2\alpha]^2\} \\ &+ q^2s^2\{2F^2\cos^2\alpha[(R^{-1} + 1)\sin^2\alpha - 2s^2] - \gamma^2(1 - F^2)\} \\ &+ s^4[R^{-1}\sin^2\alpha - s^2 - F^2\cos^2\alpha] = 0. \end{aligned} \tag{30}$$

Provided (30) has positive real roots, (an assumption which is tested against real data in Section 3), the solution gives q as a function of angle, β, except (as noted above) where $\beta = \alpha$. Figure 1 indicates that except near the critical frequency, $q = l/k$ is insensitive to the precise estimation of R, so that, in principle, good accuracy may be obtained for $k = l/q$. The sign of q is however undetermined, and some means are needed to select the appropriate sign of k in relation to the physical properties of possible wave fields (or to make additional measurements of the wave field) to resolve the ambiguity.

d. Wavenumbers and wave energy

The y-wavenumber component, l, is in the horizontal plane along the slope. Let K and M be the horizontal wavenumber component directed towards the slope and the vertical component, respectively, with

$$K = k\cos\alpha - m\sin\alpha, M = m\cos\alpha + k\sin\alpha. \tag{31}$$

An alternative form of the dispersion relation, (14), is

$$\sigma^2 = [N^2(K^2 + l^2) + f^2M^2]/(K^2 + l^2 + M^2), \tag{32}$$

or referred to the tilted (x, y, z) axes and corresponding wavenumbers (k, l, m),

$$\sigma^2 = \{N^2[(k\cos\alpha - m\sin\alpha)^2 + l^2] + f^2(m\cos\alpha + k\sin\alpha)^2\}/(k^2 + l^2 + m^2) \tag{33}$$

and this gives two possible roots for the wavenumber, m, normal to the slope:-

$$m/k = [-\sin\alpha\cos\alpha \pm \cos\beta(\sin^2\beta + q^2\gamma)^{1/2}]/\gamma \tag{34}$$

where (14) has been substituted for σ^2. Remarkably the expression is independent of F. and only the square of q appears so its sign is immaterial. The wavenumber normal to the slope, m, can be found from (34) as a function of β (or σ) using the known values of $q(\beta)$, $k(\beta) = l/q$, and α. The two roots in (34) correspond to waves which are incident or reflected from the slope at the same angle, β, to the horizontal.

Close to the boundary where measurements are made, the temperature and motion fields are affected by both the incident and the reflected waves. Which are most likely to dominate the wave spectra depend on their relative amplitudes. If, as assumed above, there is no significant loss of energy on the slope, then the wave energy flux of the incident wave will be equal to that of the reflected wave. The wave phase and group velocity are at right angles (Mowbray and Rarity, 1967), and the energy density of waves of amplitude, a, far from the slope is $\rho_0 N^2 a^2(1 + R^{-1})/2$, where R is given by (20) and, depending only on F and β, is the same for the incident and the reflected waves. Conservation therefore implies that $a^2\lambda c_g$ is conserved, where λ is the wavelength and c_g is the group velocity (Eriksen, 1982). Using expressions for the group velocity, $c_g^2 = (\partial\sigma/\partial K)^2 + (\partial\sigma/\partial l)^2 + (\partial\sigma/\partial M)^2 = (N^2 - f^2)M^2(K^2 + l^2)/(K^2 + l^2 + M^2)^3$, for $\lambda = 2\pi/(K^2 + l^2 + M^2)^{1/2}$ and substituting from the dispersion relation, (14), we find that $c_g^2\lambda^2 = (N^2 - f^2)\lambda^4 \sin^2 2\beta/(16\pi^2)$. Since β is conserved on reflection this implies that the ratio of the amplitudes of the incident and reflected waves is $a_I/a_R = \lambda_R/\lambda_I$, the ratio of the incident and reflected wavelengths. However using the wavenumber vector in the sloping coordinates, the wavelength is $\lambda = 2\pi/(k^2 + l^2 + m^2)^{1/2}$. Both k and l are conserved on reflection, so the incident or reflected wave having the greater amplitude, and which is therefore contribute most to the spectra on which the analysis is based, is that with the largest value of m^2. Inspection of (34) shows that the appropriate root is that with the *negative* sign.

The component of the group velocity normal to the slope, $c_{gn} = \partial\sigma/\partial m$, of the dominant waves can be found from (33), using (34) with the negative sign, as

$$\begin{aligned} c_{gn} = (N^2 - f^2)k^3 \cos\beta(\sin^2\beta + q^2\gamma)^{1/2}[\sin\alpha\cos\beta + \cos\alpha(\sin^2\beta + q^2\gamma)^{1/2}] \\ \times [\cos\alpha(\sin^2\beta + q^2\gamma)^{1/2} + \sin\alpha\cos\beta]/[\gamma^2\sigma(k^2 + l^2 + m^2)]. \end{aligned} \tag{35}$$

This has the same sign as k, so that if $k > 0$, $c_{gn} > 0$ and the reflected waves are dominant whilst if $k < 0$, $c_{gn} < 0$ and incident waves dominate the spectra.

Substitution of (34), again with negative sign, into (31) gives

$$\begin{aligned} K &= (k/\gamma)[\cos\alpha \sin^2\beta + \sin\alpha\cos\beta(\sin^2\beta + q^2\gamma)^{1/2}], \quad \text{and} \\ M &= -(k/\gamma)\cos\beta[\sin\alpha\cos\beta + \cos\alpha(\sin^2\beta + q^2\gamma)^{1/2}]. \end{aligned} \tag{36}$$

Since the phase and group velocities are at right angles, if $M > 0$, the wave phase advances upwards, and wave energy is downward, and vice versa. The horizontal component K

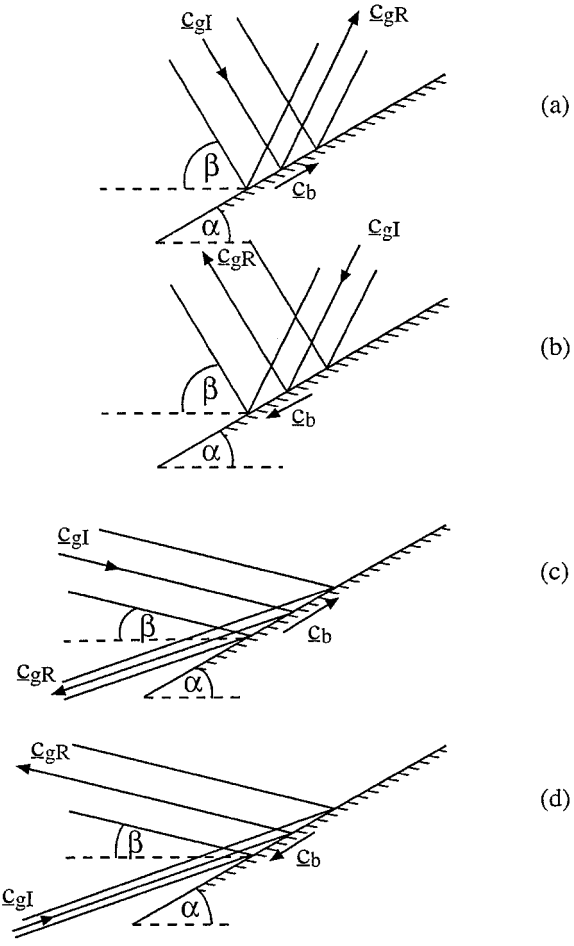

Figure 2. The reflection of internal waves from a uniform sloping boundary with incident waves having azimuthal angles equal to 0 or π. The lines represent lines of constant phase. The symbols $\mathbf{c}_{g\,I}$ and $\mathbf{c}_{g\,R}$ indicate the group velocity vectors of incident and reflected waves, respectively, parallel to lines of constant phase, and $\mathbf{c}_b$ is the direction of phase propagation on the slope. (a) and (b) show the super-critical case with $\alpha < \beta$ (and $\sigma > \sigma_c$), with (a) the incident wave having propagation towards shallow water ($\theta_I = 0$) and (b) propagation towards deeper water ($\theta_I = \pi$). In both cases the only possible incident waves have downward vertical components of group velocity and $\theta_R = \theta_I$. (c) and (d) shows the sub-critical case with $\alpha > \beta$ (and $\sigma < \sigma_c$) for incident waves with downward or upward vertical components of group velocity, respectively. In both cases $\theta_I = 0$ and $\theta_R = \pi$.

indicates the direction of both phase and energy propagation. Examples are sketched in Figure 2 which shows reflection at normal incidence. Vectors $\mathbf{c}_{gI}$ and $\mathbf{c}_{gR}$ are the group velocities of the incident and reflected waves and $\mathbf{c}_b$ (in the same direction as k) is the phase direction on the inclined plane. The lines tilted at angles β to the horizontal indicate

surfaces of constant phase. Parts a and b ($\beta > \alpha$) are supercritical waves, and c and d ($\beta < \alpha$) subcritical waves. In a, for example, the phase speed on the boundary indicated by $\mathbf{c}_b$, is up-slope so $k > 0$ and the reflected wave is dominant. Since $\gamma > 0$, (36) gives $K > 0$ and $M < 0$; the reflected wave has downward phase and upward group velocity as shown, and travels towards shallower water.

e. The azimuthal angle, θ(σ), and wave reflection

The azimuthal direction of wave energy propagation is given by the angle θ where

$$\theta = (l/|l|) \tan^{-1} (|l|/K), \tag{37}$$

where $\tan^{-1}$ is taken as an angle between 0 and π. With this choice, the azimuthal angle is positive for propagation in the y direction (l positive). When $0 < |\theta| < \pi/2$ the energy propagation is toward shallower water (with $K > 0$), whilst if $\pi/2 < |\theta| < \pi$ energy propagation is towards deeper water ($K < 0$). The azimuthal angles are limited by constraints imposed by geometry and wave propagation characteristics.

The azimuthal angle of a reflected wave, θ_R, generally differs from that of the incident, θ_I, even though their frequencies, σ, propagation directions, β, and wavenumbers on the slope, (k, l) are the same (Eriksen, 1985; Thorpe, 1999a). Since however incident and reflected waves have the same along-slope wavenumber, l, their azimuthal angles have the same sign. Sub-critical ($\gamma < 0$) and super-critical ($\gamma > 0$) waves have different properties of reflection. For super-critical waves it can be shown geometrically that, in general,

$$\theta_R = \theta_I - 2 \tan^{-1} [\tan \alpha \sin \theta_I/(\tan \beta + \tan \alpha \cos \theta_I)], \tag{38}$$

with the inverse formula

$$\theta_I = \theta_R + 2 \tan^{-1} [\tan \alpha \sin \theta_R/(\tan \beta - \tan \alpha \cos \theta_R)]. \tag{39}$$

For values of $|\theta_I| < \pi/2$, $|\theta_R| < |\theta_I|$ so that propagation is then directed more closely upslope after reflection. Propagation of the reflected wave energy toward deeper water ($|\theta_R| > \pi/2$ and $K < 0$) occurs only if $|\theta_I| > \pi/2 + 2 \tan^{-1} (\tan \beta/\tan \alpha) = \theta_{I*}$, say. This exceeds π/2, so that propagation of the reflected wave towards deeper water occurs only when the incident wave propagates with an azimuthal angle significantly greater than π/2 i.e. from relatively shallow water. Conversely, waves with $|\theta_R| > \pi/2 - 2 \tan^{-1} (\tan \alpha/\tan \beta)$ cannot result from the reflection of incident waves which carry energy towards shallower water (i.e. with $|\theta_I| < \pi/2$); they can only come from incident waves which are propagating downslope from shallower water.

For supercritical waves we may therefore adopt the following procedure. Assume first that $k > 0$ so that from (35) the dominant waves are reflected waves with $K > 0$ and $M < 0$. Estimate their azimuthal direction, θ_R, using (36) and (37) and the value of q^2 found by solving (30), provided of course that real roots are obtained. If the value of $|\theta_R|$ found is less than $\pi/2 - 2 \tan^{-1} (\tan \alpha/\tan \beta)$, then the corresponding incident waves carry energy towards the slope from deeper water and (39) can be used to determine the direction from

which they come. If however $|\theta_R| > \pi/2 - 2\tan^{-1}(\tan\alpha/\tan\beta)$, the corresponding incident waves can only have arisen from the shallower water, up-slope, direction. In some cases, for example the relatively narrow shallow water region of a lake, an energy source in shallow water may appear unlikely, but not impossible. In this case the second possibility, $k < 0$, may be explored. Here, however, the dominant waves are the incident waves and their direction, from (36), has $K < 0$ and the incident wave energy propagates from relatively shallow to deeper water, indicating a generation source up-slope of the observation position.

For *sub-critical* waves ($\gamma < 0$) with downward energy propagation

$$\theta_R = \theta_I + 2\tan^{-1}[(\tan\alpha\cos\theta_I + \tan\beta)/\tan\alpha\sin\theta_I], \tag{40}$$

with the inverse formula

$$\theta_I = \theta_R - 2\tan^{-1}[-(\tan\alpha\cos\theta_R + \tan\beta)/\tan\alpha\sin\theta_R]. \tag{41}$$

The presence of the boundary excludes incident waves with downward components of group velocity if $|\theta_I| > \cos^{-1}(-\tan\beta/\tan\alpha)$. *All* waves reflect toward deeper water, independent of whether $|\theta_I|$ is greater or less than $\pi/2$. If $0 \le |\theta_I| \le \pi/2$ (toward shallower water) then $\pi \ge |\theta_R| \ge 2\tan^{-1}[(\tan\alpha + \tan\beta)(\tan\alpha - \tan\beta)]$ and if $\pi/2 < |\theta_I| < \cos^{-1}(-\tan\beta/\tan\alpha)$ (toward deeper water), then $2\tan^{-1}[(\tan\alpha + \tan\beta)(\tan\alpha - \tan\beta)] > |\theta_R| > \cos^{-1}(-\tan\beta/\tan\alpha)$. For upward energy propagation of the incident waves, however,

$$\theta_R = \theta_I + 2\tan^{-1}[(\tan\alpha\cos\theta_I - \tan\beta)/\tan\alpha\sin\theta_I], \tag{42}$$

with the inverse formula

$$\theta_I = \theta_R - 2\tan^{-1}[(\tan\beta - \tan\alpha\cos\theta_R)/\tan\alpha\sin\theta_R], \tag{43}$$

and because of the boundary there can be no incident waves with upward energy propagation when $\theta_I > \cos^{-1}(\tan\beta/\tan\alpha)$. The reflected waves carry energy toward deeper water ($\theta_R > \pi/2$) if $\theta_I < \cos^{-1}(2\tan\alpha\tan\beta/(\tan^2\alpha + \tan^2\beta)$, but toward shallow water if $\cos^{-1}(2\tan\alpha\tan\beta/(\tan^2\alpha + \tan^2\beta) < \theta_I < \cos^{-1}(\tan\beta/\tan\alpha)$.

For subcritical waves we may first, as we did for supercritical waves, suppose that $k > 0$, so that by (35) the reflected waves dominate. Eqs. (36) give $K < 0$ and $M > 0$, so energy propagation is downward toward deeper water. The value of θ calculated from (37) gives the direction of the reflected wave, θ_R. If $\pi \ge |\theta_R| > 2\tan^{-1}[(\tan\alpha + \tan\beta)(\tan\alpha - \tan\beta)]$ then (41) gives $0 \le |\theta_I| < \pi/2$ i.e. an incident wave propagating towards shallower water, whilst if $2\tan^{-1}[(\tan\alpha + \tan\beta)(\tan\alpha - \tan\beta)] > |\theta_R| > \cos^{-1}(-\tan\beta/\tan\alpha)$, the incident wave must be travelling towards deeper water with $\pi/2 < |\theta_I| < \cos^{-1}(-\tan\beta/\tan\alpha)$. Solutions with $|\theta_R| > \cos^{-1}(-\tan\beta/\tan\alpha)$ do not correspond to physically realisable waves. We may also choose $k < 0$, implying that the incident waves dominate. Eq. (36) now gives $K > 0$ and $M < 0$, so the waves carry energy upward toward shallower water. Eq. (37) gives the incident wave azimuthal angle, θ_I, and its modulus

must be $\leq \cos^{-1}(\tan\beta/\tan\alpha)$ for it to be physically realisable. Such physical limitations limit the possible solutions in addition to others, such as the unlikelihood of waves which originate in shallower water, but do not necessarily exclude the ambiguity of sign of k.

f. The assumptions

Several tests need be made to investigate the validity of this theory when it is applied to data. The theory is valid only for values of β at which the vertical scale of the wave, $2\pi/M$ (given by 36), is much greater than the height of the current meter above the bed. The condition that the waves propagate as rays within a region in which N is constant implies that $2\pi/M$ must be much less than the vertical distance over which the buoyancy frequency changes significantly from that at the moored instrument. It is further assumed that non-linearity leading to non-sinusoidal waves and the formation of thermal fronts (Thorpe, 1999a) is small. From (17), the displacement spectrum may be found from that of the temperature fluctuations; multiplying the temperature spectrum by $[M/(dT_0/dZ)]^2$ gives the spectrum of the mean square wave steepness, $S(\beta)$. If nonlinearity is to be negligible, the wave steepness must be small and $\sigma S(\sigma)$ must have values which are $\ll 1$.

The mutual Doppler shifting of internal waves (Alford, 2001) is ignored. This may be valid if the wave-induced current fluctuations are less than the phase speeds (σ/k, σ/l) parallel to the slope of the slowest waves included in the analysis. This is again equivalent to an assumption that the steepness of the waves, to which the currents are linearly related in a first order representation, are small.

It is implicit in the analysis that at any given frequency there are 'dominant' waves. These waves have not only to belong to a narrow band of wavelengths but must travel in similar directions. Comparison may be made with waves approaching the surface wave surf zone: for periods of time short compared to the changes in the arriving waves, the wave spectrum will be dominated by particular wave trains. These will include the swell waves coming from a single, previously-occurring, distant storm and by waves actively driven by the local wind. The directional spread of each wave class will be finite but generally well-defined, although possibly less so at the highest frequencies. The times over which wave properties are 'steady' will be less than those over which wave dispersion occurring during propagation from its origin causes a frequency shift in the swell which is large compared to the swell frequency, and small compared to the time period over which the local wind changes in speed or direction. Over longer times wave spectra will be more diffuse, combining as one the effects of waves of the same frequency coming from very different directions (depending on the changes in the direction and strength of the local wind) and, perhaps, including the effect of the arrival of swell from further distant storms or the effects of wave dispersion. Similar effects will have a bearing on waves in the internal slope boundary layer. Although internal waves are inherently more complex (e.g. whilst surface waves have a single wavelength corresponding to a given period, internal waves of different wavelengths may have the same periods), the assumption that the spectra have dominant waves may be seen as being equivalent to a supposition that the time periods over which the spectra are estimated are sufficiently small in relation to the

time-scale of processes forcing the waves, supplemented by changes caused by wave dispersion in travelling from their generation source. Insufficient is known at present about the nature of internal wave propagation and dispersion (although there is suggestion that low frequency wave packets, typically with $\sigma < 2f$, may retain coherence over vertical distances comparable to the abyssal ocean depths; Thorpe, 2002), or of the nature of high-frequency wave generation in lakes, to ascertain the likely time-scale of variation in forcing or steadiness against dispersion. It should also be mentioned in passing that the lack of directional isotropy supposed here is at variance with the generally assumed isotropy associated with the Garrett-Munk spectral description of internal waves in the ocean. It is however clear that waves with all frequencies travelling in all directions will not be present simultaneously in the ocean or in a lake at any particular location and time, although given a sufficiently large sampling space and time interval, the term 'isotropy' may be a suitable way of describing the directional properties of internal waves within some frequency band and distant from the sheltering, scattering or reflecting effects of boundaries.

One other factor should be recalled in comparing the surface surf zone and the internal slope boundary layer: the extent to which wave dissipation or reflection occur. As has been explained, the amplitude of reflecting internal waves (with frequency unchanged from that of the incident waves) may be greater than that of the incident waves. The observed 'dominant' waves in this case will be reflected components, not the incident waves. Excepting non-linear interactions, there is no parallel for surface waves. The surface surf zone is characterised by energy loss, mainly at the frequencies of the incident waves (although frequency shifting can occur, for example following wave breaking over sand bars), and reflected waves rarely, if ever, have greater amplitudes than the incident.

In the next section, data obtained from Lake Geneva are used to test the application of the theory. As is subsequently proved, the lake is by no means an ideal site for such a test, but it nevertheless demonstrates the likely applicability and some of the limitations of the theory, and reveals problems which may be encountered in its use. The two periods to be analysed are selected as being in periods of relatively low winds and little convection to avoid substantial generation from the surface. They are also not at times of the passage of internal boundary or 'Kelvin' waves (Thorpe and Jiang, 1998; Thorpe and Lemmin, 1999) to avoid waves associated with their hydraulic jumps, following wave trains, or radiated waves (see Thorpe *et al.,* 1996). The length of the periods of observations, 3 and 4 days, respectively, were chosen as being long enough to estimate the spectra at inertial frequencies. Both are longer than the period of 33 hr selected in the observational study of internal waves on the sloping side of Lake Geneva by Thorpe and Lemmin (1999), where predominance of eastward travelling waves was apparent.

3. Application to observations

a. The mooring

A mooring supporting a single Aanderaa acoustic current meter 1 m above the bottom and a set of temperature miniloggers with resolution of 1 mK at 0.1, 1.1, 3.1 and 5.1 m

above the bottom was deployed at a depth of 46 m on the sloping north side of Lake Geneva south of Bouchillon in summer 2001 with the objective of testing the applicability of the analysis by using real data. The bottom slope in the area is $(12.2 \pm 1.6)°$ and isobaths are orientated in a line due east-west. The thermocline depth determined from CTD casts made during the 48 day period of the mooring deployment was 10–30 m, varying typically by about 10 m in response to the passage of westward-going and cyclonically propagating, shock-like internal 'Kelvin' waves producing downward displacements of the thermocline. Below the thermocline, the density gradient was fairly uniform, with a mean buoyancy frequency, N, of about $5 \times 10^{-3}\,s^{-1}$ at 46 m. Sensors were synchronised to sample at 2 min intervals, much smaller than the local mean buoyancy period of about 21 min. The mooring depth was selected to avoid the large changes in buoyancy frequency within the thermocline and yet shallow enough to provide the expectation of temperature and current variations sufficiently large to be well-resolved by the instruments. The height of the current meter above the bottom was also a compromise (as mentioned in section 2a) so as to be sufficiently close to avoid significant normal components of current but yet far enough to avoid substantial frictional effects. (The near-bottom mixed layer observed in CTD casts is typically at most about 1 m thick. A greater height would usually be appropriate in the deep ocean.) The local value of the Coriolis frequency, f, is $1.01 \times 10^{-4}\,s^{-1}$, giving an inertial period of 17.3 hrs.

Two periods unperturbed by the 'Kelvin' waves, were selected. The first, 'case (i)', given label (i) in subsequent figures, has a mean flow, $V = 0.022\ m\ s^{-1}$, to the west, taken as the y axis in accordance with the choice made in Section 2 (x is up-slope to the north) and $dT_0/dZ = 32.3\ mKm^{-1}$ and $N = 4.0 \times 10^{-3}\,s^{-1}$, giving $F = 0.025$. 'Case (ii)', labelled (ii), has an easterly mean flow, $V = -0.016\ m\ s^{-1}$ and $dT_0/dZ = 37.4\ mKm^{-1}$ and $N = 4.3 \times 10^{-3}\,s^{-1}$ so that $F = 0.023$. During these periods of 3 and 4 days, respectively, the winds were light, averaging 1.87 and 1.69 $m\ s^{-1}$, and directions were variable.

b. Analysis: intrinsic frequency and along slope-wavenumber, l

Figure 3a shows the potential energy spectrum, PE, for the two cases. As remarked above, the temperature spectrum, E_T, is proportional to PE. Figure 3b shows the kinetic energy spectrum, KE, and E_u, together with E_v, the spectrum of the along-slope component of current, for reference. Spectra are divided by $\rho_0/2$.

The ratio of the spectra, $R = PE/KE$, is shown in Figure 3c. As predicted, and in contrast with the ratio in deep water, the ratio is less than one for supercritical waves, decreasing as Σ increases. In contrast to the predictions of Figure 1, however, R is not equal to one at the critical frequency, possibly because significant dissipation occurs here (Eriksen, 1982, 1985). It also remains less than one in the subcritical range suggesting that q is not much less than unity. In view of the uncertainty in the spectral estimates, and consequently in their ratio, R, 'best-fit' lines are drawn for $\log R$ and only these are used in

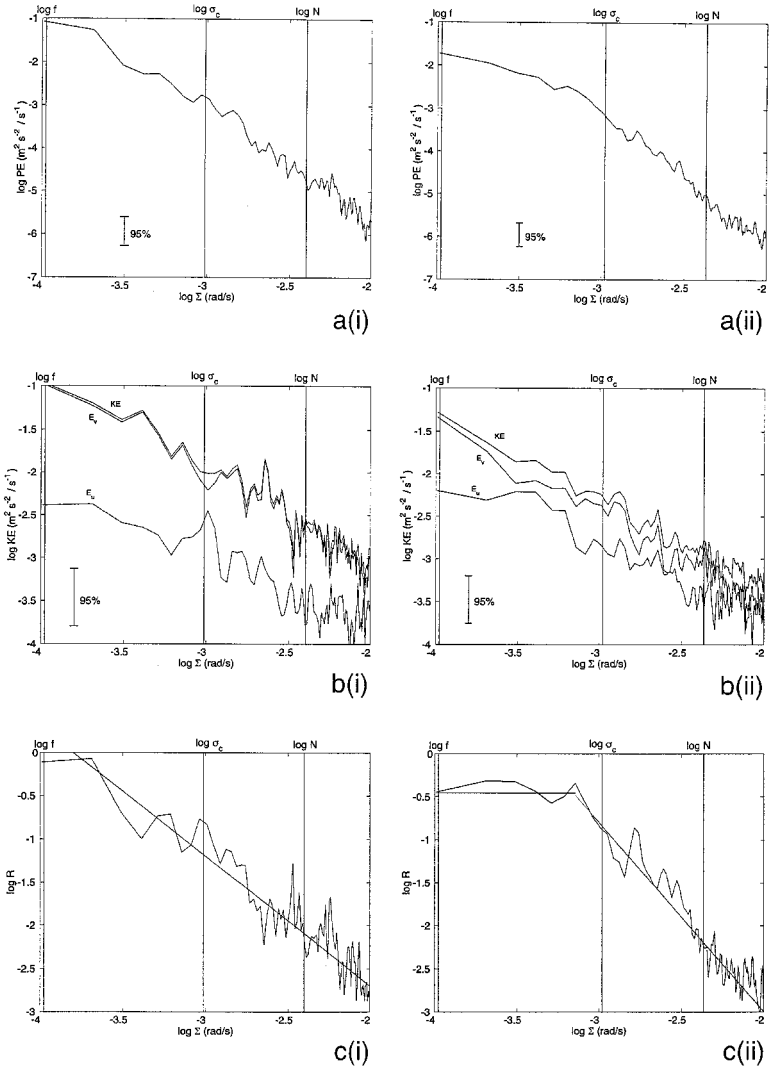

Figure 3. Observed spectra of (a) PE and (b) E_u, E_v and KE. The 95% confidence limits are shown. (c) shows the ratio, $R = PE/KE$, as a function of the measured frequency, Σ. The straight line is the best linear fit to R. Graphs with labels (i) and (ii) correspond to the two periods of analyzed data, cases one and two.

subsequent analysis. Case (ii) is fitted by two lines, one with constant R for small values of Σ, whilst in case (i) the full range is fitted by a single line.

Figure 4a shows the intrinsic frequency as a function of the measured frequency plotted on log scales, derived as explained in Section 2a and fitted, as is log R, by straight lines. In case (ii), the intrinsic frequency is only determined over a limited range, which does not

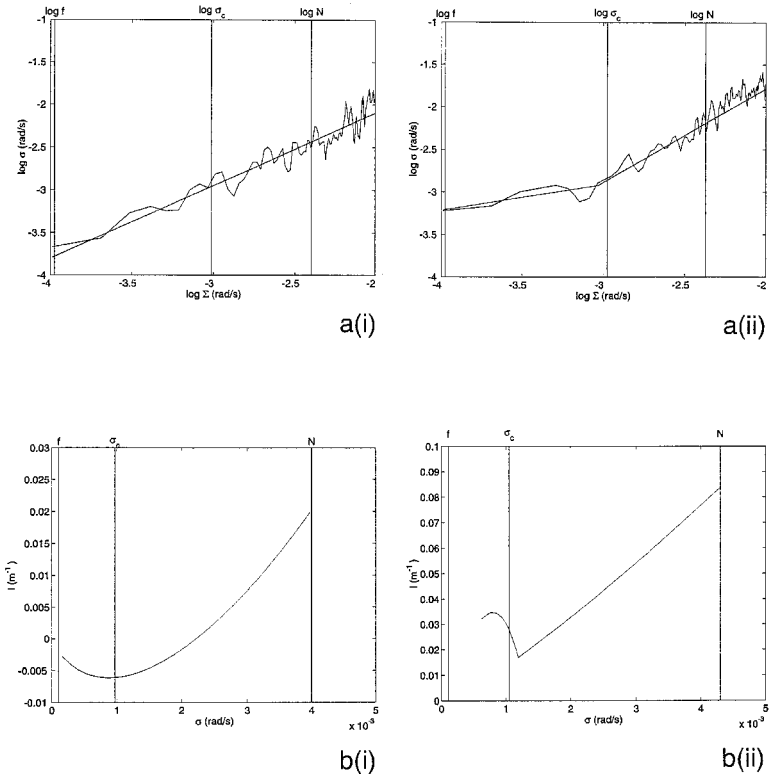

Figure 4. The variation of (a) the measured internal wave frequency, Σ, (with best-fit lines), and (b) the alongslope wavenumber, l, (in radian per sec.) with the intrinsic frequency, σ. Graphs with labels (i) and (ii) correspond to the two periods of analyzed data, cases one and two.

extend to the inertial frequency, f, because of the constant R fit in Figure 3c(ii). The along-slope wavenumber component, l, derived from (6) and from the linear fit in Figure 4a, is shown in Figure 4b. Case (i) has a range of waves propagating to the east ($l > 0$) near the critical frequency, but the waves in case (ii) are all westward-going. The estimated values of l correspond to along-slope wavelength of the waves, $2\pi/l$, which exceed 300 m in case (i) and about 60 m in case (ii). The higher frequency waves have the shorter wavelengths (greatest wavenumbers).

c. Wavenumber components k, m and M, and direction, θ_I

Eq. (30) is used to find real roots for $q = l/k$. The sign of q is unknown and, where real roots are found, they are plotted as positive values in Figure 5a versus σ. Values are found over most of the frequency range except near σ_c. The derived up-slope wavenumber component, k, $= l/q$, is also of unknown sign and is shown as positive values in Figure 5b. The estimated values of k are zero where l is zero (e.g. near σ near 2.2×10^{-3} rad.s^{-1} in case (i)).

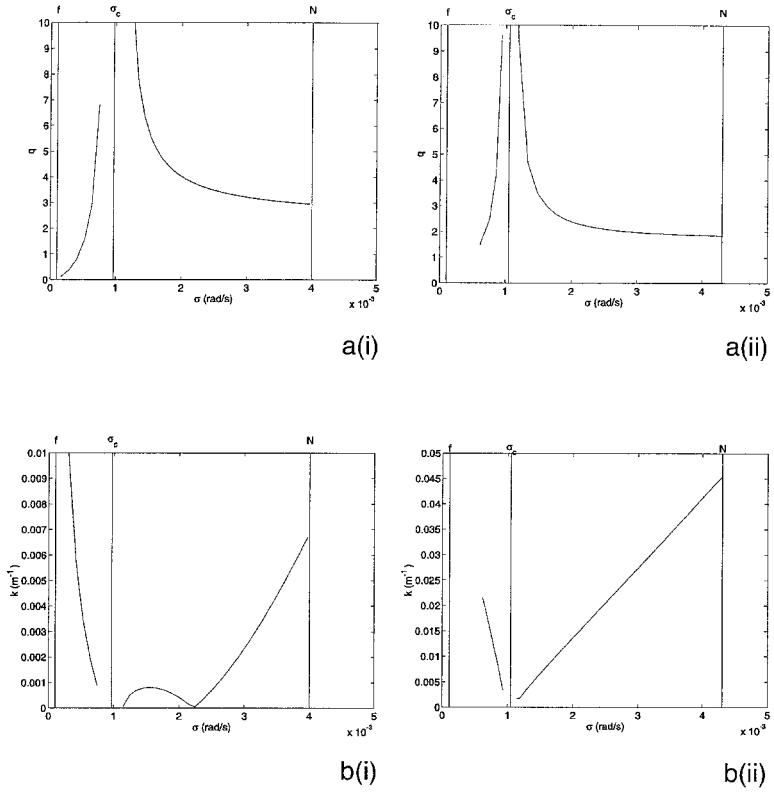

Figure 5. The variation with the intrinsic frequency, σ, of (a) the ratio of wavenumbers, $q = l/k$ (the sign can be positive or negative), and (b) the upslope wavenumber, $k = l/q$, (in radians m^{-1}. k may be positive or negative—see text). Graphs with labels (i) and (ii) correspond to the two periods of analyzed data, cases one and two.

No subcritical wave solutions are found with real values of m; the term $(\sin^2 \beta + q^2\gamma)$ in (34) is found to be always negative.

For subcritical waves it is supposed that $k > 0$ since, as explained in Section 2e only this leads to incident waves which can possibly reach the current meter from deeper water; the narrow shallower water region appears to be an unlikely source of internal waves. Figure 6a and b show the real values of m from (34) and M from (36), respectively, representing the dominant waves. These are solutions for reflected waves, and their calculated azimuth angles, θ_R, are shown in Figure 7a. In case (i), l changes sign and consequently so does θ_R, but in case (ii), $l > 0$ and consequently $\theta_R > 0$, waves propagating westward. The limiting value, $|\theta_R| = \pi/2 - 2 \tan^{-1} (\tan \alpha/\tan \beta)$ above which the corresponding incident waves can *only* have come from relatively shallow water (with $|\theta_I| > \pi/2$) is shown as a dashed line in Figure 7a. Excluding such physically unlikely waves, Figure 7b shows the possible azimuthal angles of the incident waves, θ_I, derived from (39), as a function of σ. Only the

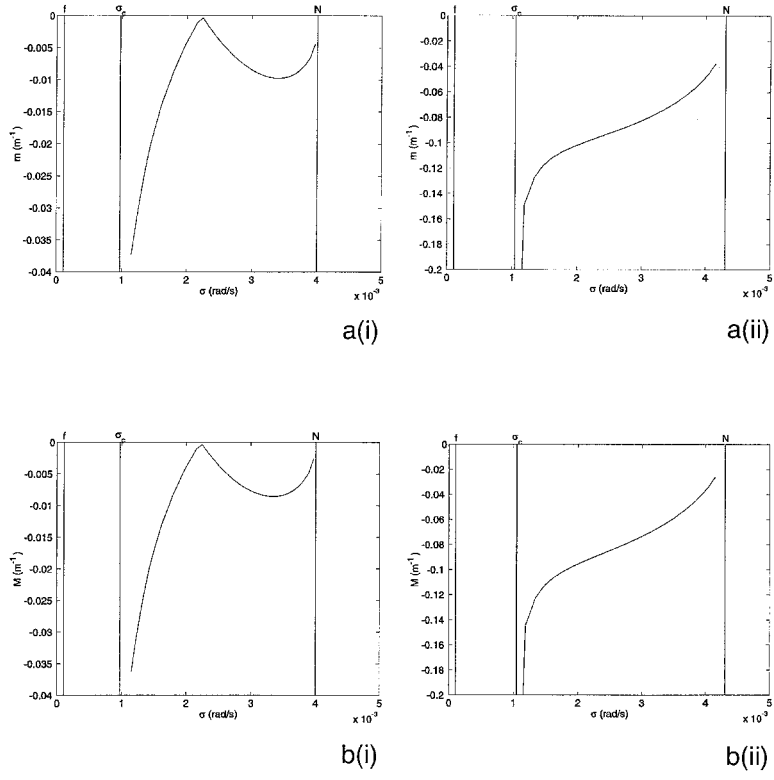

Figure 6. The variation of (a) the wavenumber normal to the slope, m, and (b) the vertical wavenumber, M, both plotted against the intrinsic frequency, σ. Wavenumbers are in radians m^{-1}. Graphs with labels (i) and (ii) correspond to the two periods of analyzed data, cases one and two.

higher frequency values are consistent with the choices made and these waves propagate with $90° > \theta_I > 60°$, or in a direction between 270°T and 300°T, within 30° of the isobaths.

d. The steepness of the waves

Figure 8 shows the spectra of σS for the two cases, plotted only in the supercritical range where realistic values of M can be estimated. Values are consistently in accordance with the assumption that non-linearities in the waves can be neglected.

4. Discussion

Given the relatively few data from the single current meter on which the analysis relies, it is hardly surprising that, in the application described in Section 3, uncertainty remains about the possible signs of wavenumbers of the waves near the slope. Ambiguity might be resolved by the addition of temperature sensors some distance above the current meter or

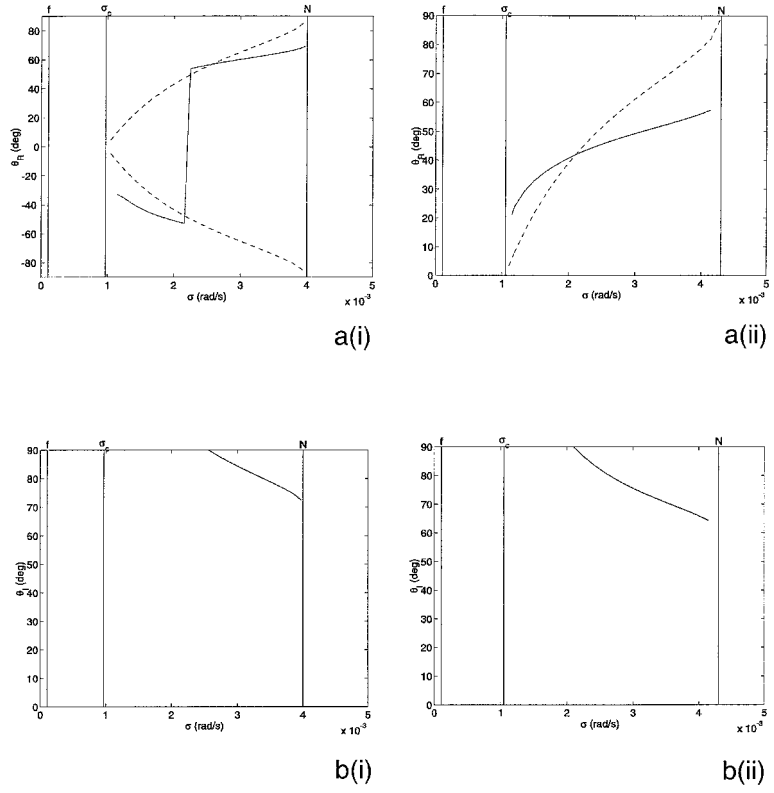

Figure 7. The variation of azimuthal angles with the intrinsic frequency, σ. (a) the supercritical reflected wave azimuth, θ_R. The dashed line shows the limiting value $|\theta_R| = \pi/2 - 2\tan^{-1}(\tan\alpha/\tan\beta)$ (expressed in degrees) above which incident waves propagate toward deeper water. (b) the supercritical incident wave azimuth, θ_I, Graphs with labels (i) and (ii) correspond to the two periods of analyzed data, cases one and two.

along the slope. It is nevertheless remarkable that so much information might, in principle, be gleaned from single point data set. In view of the failure to establish much information about waves at subcritical frequencies, shorter periods of perhaps 10 times the period of critical waves (here about 17 hrs) might still have provided useful information.

However two serious problems arise in the analysis of data. The first is that no wavenumbers, *m*, can be found for subcritical wave and the second, perhaps related problem, is that the inferred supercritical vertical wavenumbers are relatively small; the vertical wavelengths are of order 60 m or more. Whilst the necessary condition that this wavelength is large compared to the height of the current meter above the slope is well satisfied, the assumption that the buoyancy frequency is uniform over the vertical scale of the waves is violated since the thermocline is only some 25 m above the current meter which is itself only 46 m below the surface. Similarly, the largest values of *k* (Fig. 5b) are

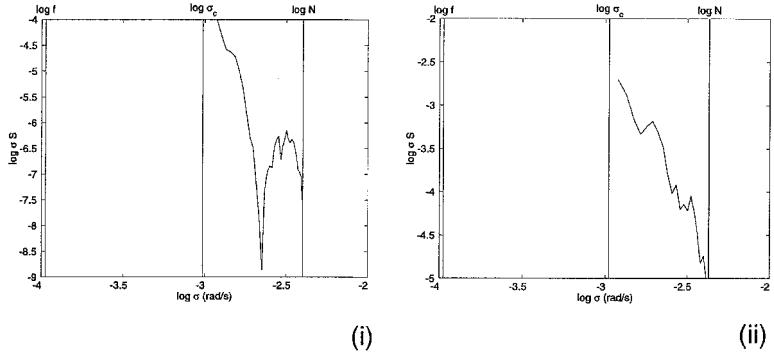

Figure 8. The spectrum of wave wave frequency times the internal wave steepness, $\sigma S(\beta)$. Graphs with labels (i) and (ii) correspond to the two periods of analyzed data, cases one and two.

about $0.045\,\mathrm{m}^{-1}$ giving minimum upslope wavelengths of 157 m. The thermocline intersects the slope at a distance about 25/sin α = 118 m upslope of the measurement location, not far enough to justify the assumption of uniformity of N. Nor is the slope smooth over the scale of the waves. The implicit assumption that the internal waves are dominated by those propagating with nonzero vertical wavenumbers as rays rather than as modes propagating on the thermocline is consequently untenable. The problems arising at the lower subcritical frequencies are also most likely because, in the lake, such wave motions are largely dominated by wave modes (Antenucci and Imberger, 2001). The along-slope wavenumbers, l, and the intrinsic frequencies are however correctly estimated using the analysis of Section 2a. The analytical method may have greater applicability in the deep abyssal ocean.

Might significant results be hidden by making the linear fits to $\log R$ and $\log \sigma$ in Figures 3c and 4a? At the kind suggestion of a referee we examined the coherence, Co, and phase of the temperature, T, and upslope velocity component, u. According to (4), T and u should be correlated with a 90° phase difference, T leading u. High coherence with appropriate phase offers a means to identify those parts of the frequency range which conform to the assumptions underlying the theory, at least of Section 2a, and to discount other parts of the frequency range. In both case periods, Co is generally low, but in each there are four peaks with $Co > 0.35$ (the largest exceeds 0.7), and each has associated phase in the range 75° to 105°. Except for those at the lowest frequencies (one subcritical and one supercritical), the frequencies at the peaks in Co are different in the two periods. Disappointingly, they are not associated with peaks in PE, KE or E_u which might indicate their association with narrow frequency band wave trains or groups. (Coherence is low at some spectral peaks, e.g. of E_u and KE at $\log \Sigma = -2.64$ and -2.66, respectively, in Fig. 3bii). Values of wavenumbers and angles derived using σ and R at the frequencies of the eight Co peaks are in general accordance with those found with the linear fit to R and $\log \sigma$; the derived vertical and upslope wavenumbers, M and k, are small. None show wave propagation from deeper water.

The application of the analysis to data naturally raises the question: "Are the observed fluctuations really caused by internal waves and described by internal wave theory?" This is a question of fundamental importance in the understanding of ocean and lake mixing and in determining whether internal wave-boundary interaction is indeed a primary cause of the observed enhanced diapycnal fluxes near sloping boundaries. In the deep ocean far from boundaries, Fofonoff (1969) concluded that the observed fluctuations within the internal wave frequency band were mainly consistent with those produced by internal waves, a conclusion supported by later consistency tests applied to pairs of moorings by Müller and Siedler (1976) and Müller *et al.* (1978), the latter using the IWEX data set. Although temperature fine structure (Phillips, 1971) was found to affect the internal wave field at small vertical wavenumber, isotropic turbulence could be rejected as being a cause of fluctuations over most of the frequency band. Similar consistency tests for internal waves have not, it seems, been tried in the vicinity of sloping boundaries where it might be expected that processes other than internal waves, such as intrusions and vortical mode (Kunze, 2001) generation, might be relatively important. As speculated in an earlier study of the internal surf zone of Lake Geneva (Thorpe and Lemmin, 1999), much of the fluctuation energy observed does not appear to be explicable solely by a superposition of linear internal waves. Not only are the non-linear effects involved in internal waves important, such as the formation of fronts, so too may be the effects of shear in both the horizontal and the vertical. The former may be associated with and perhaps lead to the formation of isopycnal eddies or vortical modes. The latter may lead to Kelvin-Helmholtz instability and mixing, the distortion of the internal wave field (Bouruet-Aubertot and Thorpe, 1998) or the formation of microfronts and the associated skewness of the temperature derivative (see for example Thorpe *et al.,* 1991; Kurien *et al.,* 2001). Further investigation is therefore required to provide an independent check of the conclusions about internal waves made using the analysis of Section 2. Bounds of the along-slope wavenumber component, l, might be estimated from an array of miniloggers placed along the slope. A second current meter deployed, say, 100 m along the slope from the first would provide a check of how robust were the estimates made at one instrument, and the consistency relations derived in mid-water might be applied to test the extent to which the fluctuations conform to internal waves near sloping boundaries.

The main purpose of this study is not to convince the reader that dependable information about the internal wave field can be obtained from measurements at just a single point. In view of the present results, it would not be prudent to rely on such measurements. The purpose is to identify and to draw attention to some of the yet unquantified features of internal waves and the internal slope boundary layer, particularly those described above or mentioned in the discussion in section 2f, which may affect the mixing of the deep ocean.

Acknowledgments. The authors appreciate the valuable comments of the referees. Data were kindly provided by Dr U. Lemmin. SAT is grateful for the support of the LRH, EPFL, Lausanne, Switzerland and the opportunity to collaborate with his friends there.

REFERENCES

Alford, M. H. 2001. Fine-structure contamination: observations and a model of a simple two-wave case. J. Phys. Oceanogr., *31,* 2645–2649.

Antenucci, J. P. and J. Imberger. 2001. Energetics of long internal gravity waves in large lakes. Limnol. Oceanogr., *46,* 1760–1773.

Bouruet-Aubertot, P. and S. A. Thorpe. 1998. Numerical experiments on internal gravity waves in an acceklerating shear flow. Dynamics Atmos. Oceans, *29,* 41–63.

Dunkerton, T. J., D. P. Delisi and M-P. Lelong. 1998. Alongslope current generated by obliquely incident internal gravity waves. Geophys. Res. Letts., *25,* 3871–3874.

Eriksen, C. C. 1982. Observations of internal wave reflection off sloping bottoms. J. Geophys. Res., *87,* 525–538.

—— 1985. Implications of ocean bottom reflection for internal wave spectra and mixing. J. Phys. Oceanogr., *15,* 1145–1156.

—— 1998. Internal wave reflection and mixing at Fieberling Guyot. J. Geophys. Res., *103,* 2977–2994.

Fofonoff, N. P. 1969. Spectral characteristics of internal waves in the ocean. Deep-Sea Res., Suppl., *16,* 59–71.

Gill, A. E. 1982. Atmosphere-Ocean Dynamics. Academic Press, London, 662 pp.

Imberger, J. and G. N. Ivey. 1993. Boundary mixing in stratified reservoirs. J. Fluid Mech., *248,* 477–491.

Kunze, E. L. 2001. Vortical Modes, Encyclopedia of Ocean Sciences, *6,* J. H. Steele, S. A. Thorpe and K. K. Turekian, eds., Academic Press, London, 3174–3178.

Kurien, S., K. G. Aivalis and K. R. Sreenwasan. 2001. Anisotropy of small-scale turbulence. J. Fluid Mech., *448,* 279–288.

Lazier, J. R. N. 1973. Temporal changes in some fresh water temperature structures. J. Phys. Oceanogr., *3,* 226–229.

Ledwell, J. R. and A. Bratkovich. 1995. A tracer study of mixing in the Santa Cruz Basin. J. Geophys. Res., *100,* 20,681–20,704.

Ledwell, J. R. and B. M. Hichey. 1995. Evidence of enhanced boundary mixing in the Santa Monica Basin. J. Geophys. Res., *100,* 20,665–20,679.

MacCready, P. and G. Pawlak. 2001. Stratified flow along a corrugated slope: separation drag and wave drag. J. Phys. Oceanogr., *31,* 2824–2839.

Morris, M. Y., M. M. Hall, L. L. St-Laurent and N. Hogg. 2001. Abyssal mixing in the Brazil Basin. J. Phys. Oceanogr., *31,* 3331–3348.

Mowbray, D. E. and B. S. H. Rarity. 1967. A theoretical and experimental investigation of the phase configuration of internal waves of small amplitude in a density stratified fluid. J. Fluid Mech., *28,* 1–16.

Müller, P., D. J. Olbers and J. Willebrand. 1978. The IWEX spectrum. J. Geophys. Res., *83,* 479–500.

Müller, P. and G. Siedler. 1976. Comsistency relations for internal waves. Deep-Sea Res., *23,* 613–628.

Phillips, O. M. 1971. On spectra measured in undulating layered medium. J. Phys. Oceanogr., *1,* 1–16.

Thorpe, S. A. 1992. Thermal fronts generated by internal gravity waves reflecting from a slope. J. Phys. Oceanogr., *22,* 105–108.

—— 1996. The cross-slope transport of momentum by internal waves generated by along-slope currents over topography. J. Phys. Oceanogr., *26,* 191–204.

—— 1997. On the interactions of internal waves reflecting from slopes. J. Phys. Oceanogr., *27,* 2072–2078.

—— 1999a. Fronts formed by obliquely reflecting internal waves at a sloping boundary. J. Phys. Oceanogr., *29,* 2462–2467.

—— 1999b. The generation of alongslope currents by breaking internal waves. J. Phys. Oceanogr., *29,* 29–38.

—— 1999c. 75 + 25 = 99 ± 1, or some of what we still don't know: wave groups and boundary processes, *in* Proceedings, "Aha Huliko'a Hawaiian Winter Workshop, Dynamics of Oceanic Internal Gravity Waves, II," P. Muller, ed., SOEST Special Publication, 129–136.

—— 2001a. On the reflection of internal wave groups from sloping topography. J. Phys. Oceanogr., *31,* 3121–3126.

—— 2001b. Internal wave reflection and scatter from sloping rough topography. J. Phys. Oceanogr., *31,* 537–553.

—— 2002. On the dispersion of pairs of internal inertial gravity waves. J. Mar. Res., *60,* 461–476.

Thorpe, S. A., M. Cure and M. White. 1991. The skewness of temperature gradients in oceanic boundary layers. J. Phys. Oceanogr., *21,* 428–433.

Thorpe, S. A. and R. Jiang. 1998. Estimating internal waves and diapycnal mixing from conventional mooring in a lake. Limnol. Oceanogr., *43,* 936–945.

Thorpe, S. A., J. M. Keen, R. Jiang and U. Lemmin. 1996. High frequency internal waves in Lake Geneva. Phil. Trans. R. Soc. Lond. A, *354,* 237–257.

Thorpe, S. A. and U. Lemmin. 1999. Internal waves and temperature fronts on slopes. Ann. Geophysicae, *17,* 1227–1234.

Toole, J. M., R. W. Schmitt and K. L. Polzin. 1997. Near-boundary mixing above the flanks of a midlatitude seamount. J. Geophys. Res., *102,* 947–959.

Zikanov, O. and D. N. Slinn. 2001. Along-slope current generation by obliquely incident internal waves. J. Fluid Mech., *445,* 235–261.

Received: *23 April, 2002;* revised: *5 November, 2002.*